An Analytical Heat Wave Definition Based on the Impact on Buildings and Occupants

Key words: heat wave, buildings, super-synthetic weather.

ABSTRACT

Alongside a mean global rise in temperature, climate change predictions point to an increase in heat waves and an associated rise in heat-related mortality. This suggests a growing need to ensure buildings are resilient to such events. Unfortunately, there is no agreed way of doing this, and no standard set of heat waves for scientists or engineers to use. In addition, in all cases, heat waves are defined in terms of external conditions, yet, as the Paris heat wave of 2003 showed, people die in the industrialised world from the conditions inside buildings, not those outside. In this work, we reverse engineer external temperature time series from monitored conditions within a representative set of buildings during a heat wave. This generates a general probabilistic analytical relationship between internal and external heat waves and thereby a standard set of events for testing resilience. These heat waves are by their simplicity ideal for discussions between clients and designers, or for the setting of national building codes. In addition, they provide a new framework for the declaration of a health emergency.

1 Introduction

The IPCC has confirmed that extreme weather events will be more severe and more frequent in the near future (IPCC, 2014). Unfortunately, there exist little knowledge about how these events, be they heat waves or cold snaps, will affect buildings. Common practice is to evaluate the response (the internal conditions) of single buildings via the running of complex simulations using typical, or near typical, weather (Jentsch et al. 2008; Guan 2009; Eames et al. 2011; Kershaw et al. 2011). Although this is relatively accurate for calculating annual energy demand and general thermal comfort, it has little to say with respect to morbidity during an extreme event like a heat wave.

Historically, heat waves that kill are by their nature infrequent and this makes statistical analysis of their properties difficult. Unfortunately, their consequences can be extreme, with the European heat wave of 2003 causing over 14,000 deaths in Paris alone (Stott et al. 2004), and even more small-scale events like the July 2006 heat wave, which killed 107 in Porto, are of growing concern (Monteiro et al. 2013). Considering that heat waves are going to become more frequent and severe (Meehl and Tebaldi 2004), the understanding on how they affect buildings is clearly not just an academic question, but important for accessing society-wide resilience, and the scale of the response.

Very sensibly, different countries have defined heat waves in different ways. This localised response makes sense as different locations have different: mean temperatures, temperature time series, and levels of adaption amongst their population. For example, one of the oldest definitions is that of A. T. Burrows who defined a heat wave as a period of three days of more in which the daily maximum temperature exceeds 32.2ºC. This would clearly not work in Madrid, Spain where the average daily maximum temperature in August is 32 ºC. Table 1 shows some of the resultant diversity.

Table 1. Example heat wave definitions. (Robinson 2001).

Country	Temperature	Time	Definition	Reference
Netherlands	> 25ºC & >30ºC	>= 5 days punctual	More than 4 days with a mean temperature higher than 25 and reaching 30ºC	(DMI 2013)
Denmark	Average maximum >28ºC	>= 3 days	More than 2 days with mean max temperature higher than 28ºC	(DMI 2013)
Sweden	>25ºC	>=5 days	More than four days with temperatures higher than 25ºC.	(SMIH 2013)
US (Northeast)	> 32.2ºC	>=3 days	Temperature reaches or exceeds 32.2ºC during three days	(NWS, 2019)
US California	> 37.8ºC	>=3 days	Temperature reaches or exceeds 37.8ºC during three days	(NWS, 2019)
South Australia	>35ºC or 40ºC	>=5 days Or 3 days	5 days with a temperature higher than 35ºC or three higher than 40ºC	(BOM 2013)

In the UK two definitions are in frequent use: (a) when the daily maximum temperature on more than five consecutive days exceeds the average maximum temperature by 5 °C; (b) the other is dependent on the region, but typically when the predicted temperature is 30 °C by day and 15 °C overnight for at least two consecutive days. The definition given in (a) heavily influences the thoughts presented in this paper.

Russo et al. (2015) developed a methodology that defines a heat wave as an intensity factor based on the typical weather at the location (Russo et al.), which was then used to show that in many areas of Europe heat waves are becoming more common (Zampieri, Russo et al. 2016). However, the health impacts of extreme temperatures depend on both the situation relative to the historic norm, and to absolute values. It is worth noting that the absolute (i.e. non-relative) limits give in Table 1 are still somewhat relative to the historic situation, with for example higher values in southern rather than northern California.

In all these cases the heat wave is defined using external conditions. However, as the Paris heat wave of 2003 showed, it is internal conditions that lead to issues of thermal comfort

failure, morbidity and death. It is therefore reasonable that we try to define a heat wave in terms of the likely conditions within the building stock.

As different buildings respond differently to any external temperature time series, such a definition would most likely be framed as the likely production of excessive conditions in some fraction of buildings, for example at least 10% of buildings expecting to have a temperature above 28 degrees during 3 days. In addition, it would be biased towards the types of buildings in which vulnerable occupants struggle to deal with the thermal environment and die. However, basing a definition of a heat wave on likely internal conditions forces us to find a way of relating the external conditions to the internal conditions. Given the external time series it is possible to find the internal temperature series using dynamic simulation of the stock. However, this process is not reversible, as required here, where we need to find the external times series that led to particular conditions within the stock. This paper investigates if it is possible to create a methodology that achieves this and should be contrasted with work such as Coley and Kershaw 2010, which simply looked at how internal temperatures might rise in general as the climate warms.

A definition based on likely internal conditions in a set fraction of the building stock would be extremely useful to those wishing to justify the declaration of a heat wave in order to mobilise a public health response. It would also be useful to those looking at ways to study the resilience of the current stock, or the impact of heat waves on new designs, via the use of dynamic thermal models of buildings. Such models need a description of the weather conditions they are exposed to, typically represented in weather files that describe key information about the location and the time series of relevant weather variables. For current weather, these weather files are built using historical weather data, whereas for future weather two different approaches have been proposed: morphing and weather generators. Morphing transforms historical weather data according to a series of mathematical models that describe the expected changes in the climate (Jentsch, James et al. 2013), whereas weather generators create synthetic weather by direct weather simulation (Eames, Kershaw et al. 2011). Regardless of the approach, it has been shown that weather files need to be specific to the location of a building to generate reliable performance estimates (Eames, Kershaw et al. 2011, Liu et al. 2017).

Due to their very nature, cold snaps and heat waves are infrequent weather events, and they may or may not be present in a location's historical weather dataset. This is especially true for those events associated with increased mortality. Assuming one or more instances of such events are present in the weather records, they would be but particular realisations, unique in

their temporal signature. For instance, one heat wave might have been hotter in its maximums around the central days of the event, whereas another might have developed equally hot days over a longer period of time. This prevents in principle a robust characterisation or classification of these events in terms of their likely impact to building occupants, which in turn precludes systematic studies on how to deliver resilient buildings.

To solve this issue, it is necessary to first reflect on the purpose of the dynamic thermal simulation of buildings. It is tempting to think that they predict future internal conditions, however as the weather file (time series) used is historic, or synthetic, it will never match any future real weather the building will be exposed to, and even if it did, it would be only one year of the many the building will experience over its lifetime. In addition, as a dynamic simulation produces results every time step, there is the need to summarize these results with a set of much reduced metrics for the results to be of use, for example the maximum temperature reached or the number of hours in a year above some set temperature. Once given such information, the researcher or designer can reflect on the seriousness of the situation with respect to human health or energy use, and then consider design alternatives. This suggests that the hour-by-hour fidelity of a time series of weather is a poor way to judge a weather file. Rather, consideration should be given to its usefulness in providing a metric. This utility-based argument is given further weight by the many other hard-to-define time series that form inputs to any dynamic simulation, for example occupancy, window use or electrical gains. These time series are different for every household, rarely the same for each day, and the hour-by-hour future values for any building, let alone a whole stock, unknown, as technology and preferences and occupants will change. In these cases, modellers and practicing engineers typically use simple repeating functional forms.

These considerations suggest one possible approach to producing weather time series of future extreme weather would be to identify a heat wave as a positive distortion of a oscillatory base temperature. This could be done with a weather file that contains consecutive extrusions that grow in intensity. Climate change projections could then provide the return period of any particular event for that region. We term such files *super-synthetic* weather files as they are both synthetically created and simplified to a simple oscillatory function. The main advantage of using simple sinusoidal waveforms is that, when combined with the right models, they have analytical solutions, providing direct equations that can be reversed to provide external conditions for a given set of internal conditions. This means that rather than defining a heat wave in terms of external conditions, it would be possible to produce a temporal time series that would, for example, produce a temperature rise of greater than X for more than Y hours in Z percent of the stock.

Several questions now arise, (i) what do we use to represent the base sinusoidal temperature time series that reflect typical conditions, (ii) how do we estimate the size and length of the heat wave excursions from this, (iii) how do we represent the other weather variables? To answer these, data from real buildings (including gains and internal and external temperatures) were combined with Lump Parameter Models (LPM) and inverse modelling (Madsen and Holst 1995).

2 Methodology

The central methodology of this paper consists of reverse engineering heat waves that will have a given effect on the building stock. For this, the need for a general building model capable of responding to a time series of temperatures, yet with an analytical solution, points to the use of Lumped Parameter Models (LPMs). In order to define the parameters of these models, which equate to U-values etc., one requires a measured time series of the response of the real buildings to external driving forces. Finally, given such validated models and their parameters it is possible to estimate the impact of a sinusoidal heat wave by analytical means. It is important to understand that what is being suggested is not the creation of thermal models from a list of construction details (such as U-values and infiltration rates), which may or may not be correct, and assumed occupant behaviours, but the derivation of these from the measured times series of temperatures etc. in the buildings.

2.1 Model topology

Lumped parameter models are linear dynamic models that are sometimes referred to in building modelling as RC-networks. LPMs have analytical solutions when driven by simple inputs such as impulses or sinusoidal time series. The LPM topology (i.e. the number of components and the order of the model) can be fixed by considering the physics of the problem at hand. It has been proven in the literature that third order LPMs (with three differential equations) can be used to accurately represent buildings (Ramallo-Gonzalez et al 2015).

The parameters of the LPM can then be obtained using inverse modelling (as in Ramallo-González et al. 2018) using an observed time series of the inputs and the internal temperature time series. In our case, we use data from dwellings monitored over a summer (2006) that included a heat wave. The fact that the data used contained a heat wave is advantageous, as LPMs are linear models and therefore could lose accuracy when being operated with inputs largely different to those with which they have been trained with, particularly phenomena that are non-linear (e.g. radiation or ventilation). For example, if an LPM was trained with an average

summer, then the outcome could be accurate in periods with “normal” temperatures, but possibly become less accurate under a heat wave.

This approach should be contrasted with other methods that use approximate knowledge of building components such as U-values etc. from architectural data to build models of existing buildings. Although these methods have other advantages, such as the possibility of using more complex simulations that represent more phenomena (e.g. separate thermal bridges, or moisture transfer), they suffer from a lack of certainty of the actual U-values etc. found in the building.

For this paper a fully empirical approach was taken. Data recorded in 28 real domestic buildings (of varying architecture, form, scale and occupancy—see Appendix 1—during the summer of 2006 (May to October), are used to give a framework capable of finding the parameters of 28 LPMs that fit the observed internal temperature time series. More houses and more locations would have improved the study. However, our main focus is on demonstrating the method. Additional homes can be added whenever the data becomes available. Hopefully the introduction of the Internet of Things to buildings and the proliferation of smart meters will ensure more data soon becomes available.

2.2 Real world data

The data (see CT, 2011 for a more detailed description), contain time series of internal temperature, external temperature and electricity use at 5 minutes’ intervals in 28 UK homes situated in Manchester (3 homes) Nottingham (2), Cambridge (5), Derby (1) and Belfast (17).

Solar radiation was not included in the data set. However, as it is an important factor to evaluate the internal temperature of buildings in summer, the algorithm of Muneer was used (Muneer 1990). With it, it was possible to generate hourly series of horizontal irradiance derived from the MIDAS repository. The data generated with the Munner model, may not be as accurate during a heat wave (as this is by definition an exceptional event). However, as the LPM of the building is fitted to reproduce the real input data from the building, it is expected that when data simulating a heat wave is passed through the LPM the results will be realistic.

2.3 Reduced model

The literature shows different LPMs for specific applications (Coley and Penman 1992, Fraisse et al. 2002, Ménézo et al. 2002, Xu and Wang 2007, Malisani et al. 2010, Bacher and Madsen 2011). As the problem at hand did not have specific requirements on model complexity, but the sole goal of providing an accurate temperature response, a third order model, as the one used by Ramallo-González, was used (Ramallo-González et al, 2018), Figure 1. k_1, k_2, k_3, and k_4

are heat pathways; C_1,C_2 and C_3 are heat capacitors; $T_o(t)$ is the external temperature at time t, $T_w(t)$ is a virtual temperature of the interior of the thermal envelope (see Ramallo-Gonzalez et al 2013), $T_i(t)$ is the temperature of the internal air, $T_{TM}(t)$ is the temperature of a virtual node representing the internal thermal mass of the building (see Tindale 1993 for further details) and $g_e(t)$ and $g_s(t)$ are heat sources (represented as current sources), being the electric gains and the solar gains respectively. As the solar gains are given in terms of the global horizontal irradiance at the location, an extra factor, f, is needed to account for the smaller fraction of incident solar energy actually entering the building. A constant f value implies that the solar access to the building and shadowing can be considered fixed, which is somewhat unrealistic. However, it should be noted that heat waves in the UK are concentrated during a three-month period, during which the solar trajectory changes little. In addition, it is hard to see how the method as it stands could be expanded to include a variable f, hence this is a utilitarian assumption.

The experience of temperature within a space is a combination of the air and radiative temperatures. In our case, we have only considered as an output the air temperature as this is the one being captured by the sensors. Nevertheless, the rad-air temperature in within the LPM, but it is not reported as an output.

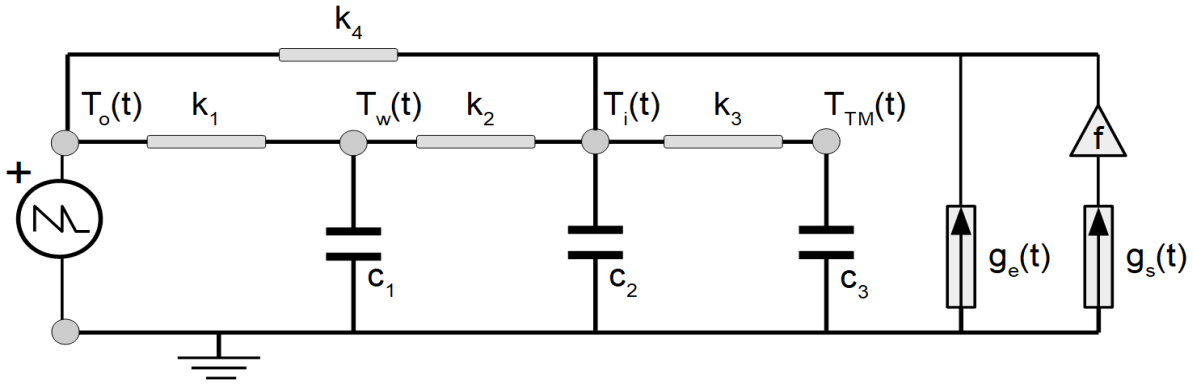

Figure 1. LPM of the methodology of this paper. T represents temperature (degree), k admittance (W/K), c capacitance (Wh/k), t time (hour) and g gains (W). The subscripts o, w, i, e, s and TM represent outside, wall, inside, environmental, surface and thermal mass respectively.

This network can be represented mathematically with the so-called state-space matrix equation (Eq. 1).

$\dot{\vec{x}}(t) = \boldsymbol{A}\vec{x}(t) + \boldsymbol{B}\vec{u}(t);$ $y(t) = \boldsymbol{C}\vec{x}(t) + \boldsymbol{D}\vec{u}(t)$	Eq. 1

where $\boldsymbol{A}$ is the system matrix, $\boldsymbol{B}$ is the input matrix, $\boldsymbol{C}$ is the output matrix, $\boldsymbol{D}$ is the feedthrough matrix, $\vec{x}$ represents the state vector, $\dot{\vec{x}}$ is the temporal derivative of $\vec{x}$, y the output vector and $\vec{u}$ the input vector.

2.4 Estimation of model parameters

The primary aim of the LPM models used in this paper is not the identification of the parameters (i.e. the resistances and capacitances of Figure 1), for thermal diagnostics of the building (as in Bacher et al. 2014, or Ramallo-González et al. 2018). Instead, we aim for models that focus on the fidelity of the internal temperature time series. This is similar to the approach found in (Coley and Penman 1998) and uses the Root Mean Square Error (RMSE) between the observed and simulated internal temperature to drive the discovery of the unknown parameters.

For model fitting we use the observed external temperature, (derived) solar gains, observed electrical gains and observed internal temperature and ignore other minor gains such as occupants' metabolism as they can be considered an order of magnitude smaller in traditional buildings (de Wilde and Tian 2009). The parameters searched were the thermal conductivity of the envelope k_1, k_2 and k_4; the thermal capacity of the thermal envelope C_1, the thermal conductivity of the thermal mass k_3, the thermal capacity of the thermal mass C_3; and the thermal capacity of the space C_2. The effect of solar gains was evaluated via f and g_s. The values discovered for each dwelling are given in Appendix 2. The RC-networks have been assumed to be time-invariant, i.e. the values of the capacitances and resistances for any building do not change during the simulation period. Since k_4 includes ventilation losses and gains which might vary as the occupants increase ventilation by opening windows further as a response to increasing internal temperatures, then close them when external temperatures are very high, the assumption of time-invariance will introduce an error in the model. Nevertheless, one has to take into consideration the impossibility of guaranteeing occupants takes complex appropriate action, so our stance is in some way precautionary. The effect of occupants in buildings can be seen for example in Pilkington et al. 2011.

However, this can be seen as a conservative approach to the model, as it ensures instances of high indoor temperatures will tend to be lower in reality than predicted by the model. This conservative approach is also necessary since it is known that households most vulnerable to high temperatures are also the least likely to operate windows, often due to mobility issues (Vellei et al. 2018). Hence the assumption of stationarity represents an important precautionary position. This assumption is also normal practice in RC-network modelling of buildings (Ramallo-González et al, 2018).

The accuracy provided by the network generated for each of the 28 buildings was examined first using visual inspection (Figures 2, 3, 4 and 5 show examples for two buildings); and secondly using Cooling Degree Hours (CDH) calculated over 18.8 degrees of the simulated (fitted) and real internal temperature, as we are interested on quantifying the error in terms of the difference in the temperature, and in terms of how much that difference is extended over time, particularly for hot periods. In all cases the fitting was highly satisfactory with an average error of 4.2% over the calculated CDH (See Appendix 2 for more details), and a worst case difference of 13%. Appendix 2 gives the error and the parameters of the Empirical Cumulative Probability Distribution (ECPD) for all 28 buildings.

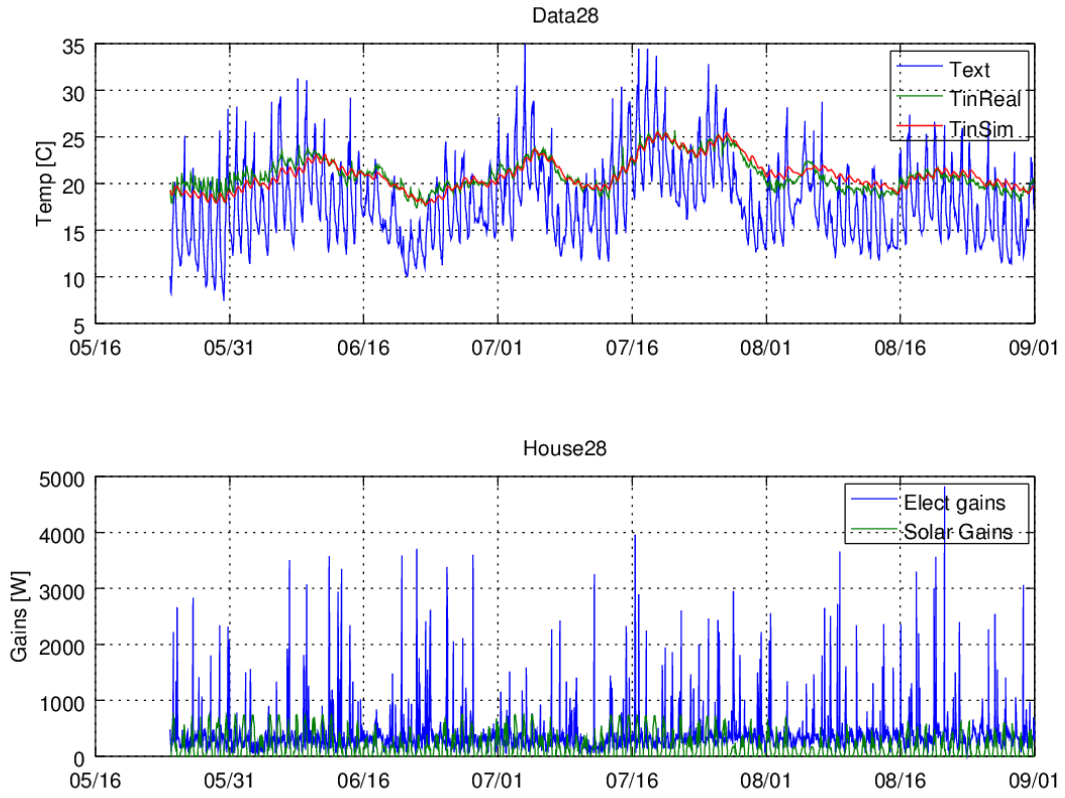

Figure 2: Three months of data for one building with a small daily temperature swing. Top, temperature time series; bottom driving forces. The reader is referred to the online version of the paper for colour graphs. T_{ext} is the external temperature; T_{in} the internal temperature (Sim indicating simulated by the LPM, Real indicating the measured internal temperature).

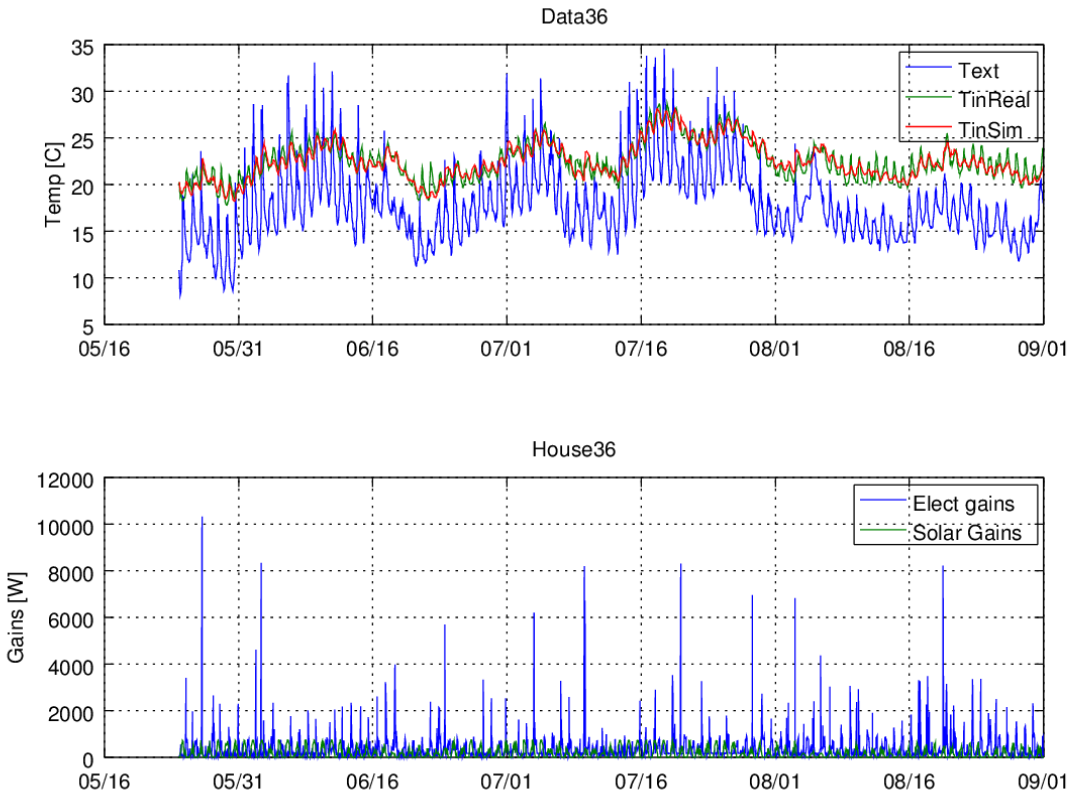

Figure 3: Building with a large daily temperature swing Top, temperature time series; bottom driving forces. The reader is referred to the online version of the paper for colour graphs. T_{ext} is the external temperature; T_{in} the internal temperature (Sim indicating simulated by the LPM, Real indicating the measured internal temperature).

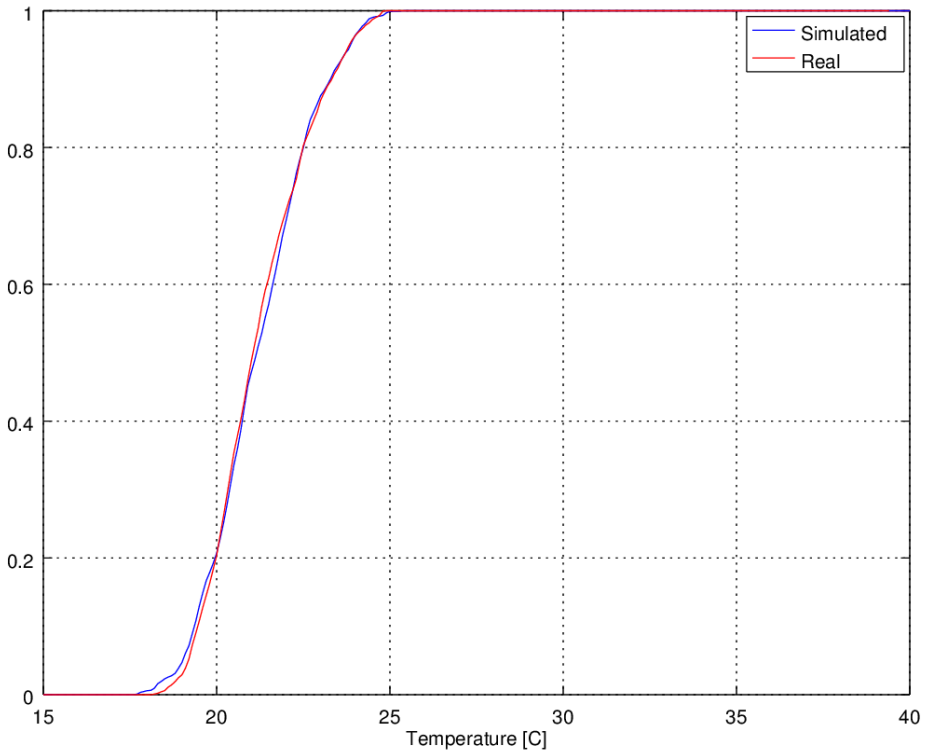

Figure 4: Example of ECPD of the real and LPM-simulated internal temperature for the building with the smallest error in CDH over 18.8 degrees between real and simulated.

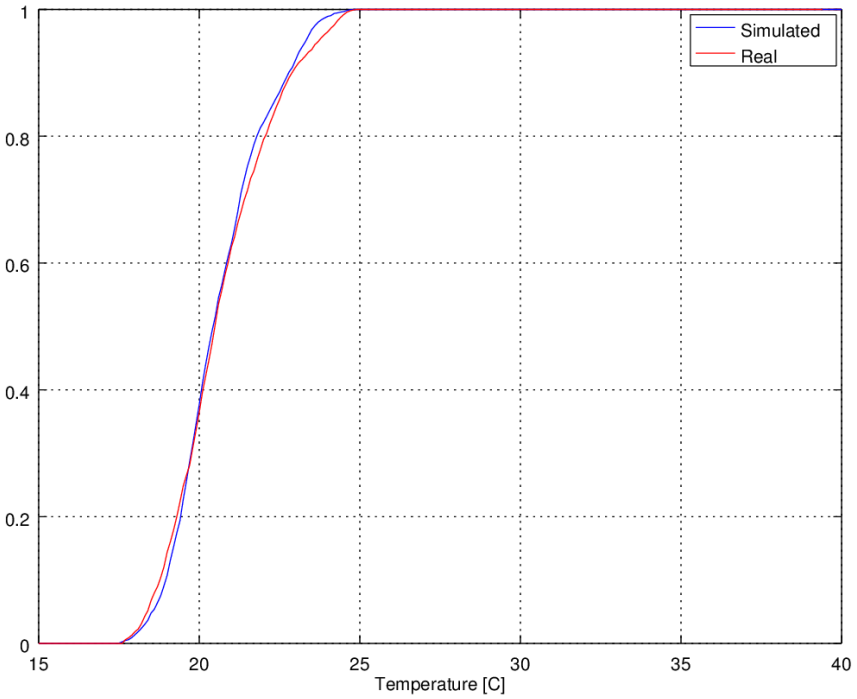

Figure 5: ECPD of real and LPM-simulated internal temperature for the building with the least good match between real and simulated.

2.5 Quantitative analysis of the impact of the gains on overheated homes

One of the reasons for modelling the buildings with a linear system is because the output from a sum of driving forces is equal to the sum of the outputs from each independent driving force. This allows one to estimate how much of any overheating is from any driving force (electrical, solar, external temperature) for each of the 28 homes of the sample.

To achieve this, each one of the LPMs representing the real buildings was simulated three times, each simulation using only one driving force i.e.: external temperature, electrical gains and solar irradiance. The results are shown in Figure 6 and Table 2. This should be studied in conjunction with the values in Appendix 2. There one can see how the parameters of the LPM representing the conductivity of the envelope are in general orders of magnitude higher than the solar factor. Also, the capacitance of the internal air of the dwelling (C_2) and the capacitance of the thermal mass C_3 provide a substantial smoothing of the driving forces applied to the internal part of the house.

We see with this that the impact of the electrical gains and solar gains would be small during the heat wave, and hence can only play a minor role in the additional rise in temperature of the building during the heat wave. It should be mentioned here, that the houses under study do not have electrical air conditioning and therefore higher temperatures do not imply higher electricity consumption. Also, a heat wave of 5 or 7 days is not enough to have a significantly different solar acceptance, which also points to the small effect that the two driving forces will have on the internal temperature rise during a heat wave.

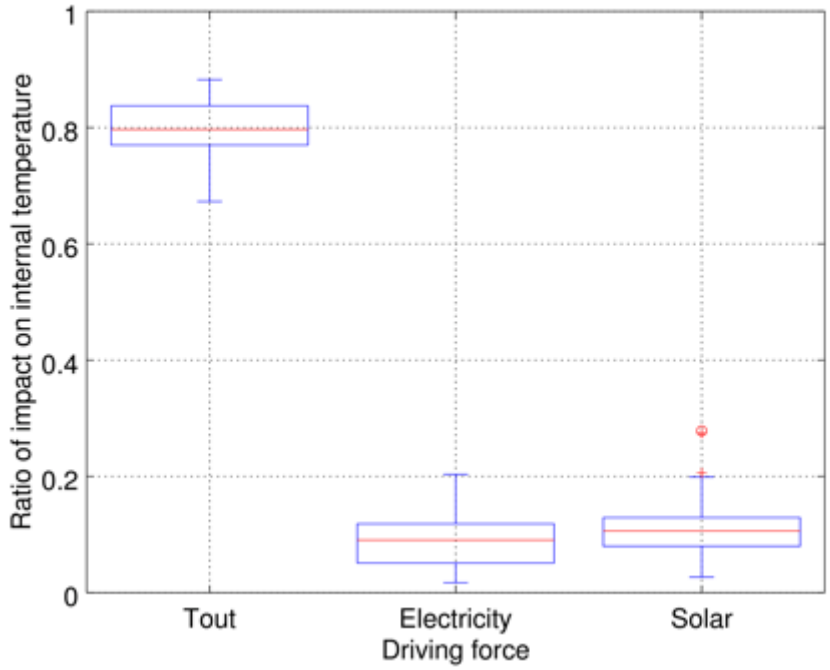

Figure 6. Influence on the internal temperature of each main driving force on the Summer of 2006.

Table 2. Quartiles of ratios of influence from the three main driving forces on internal temperature during Summer 2006 for the 28 buildings.

[No units]	Outside Temperature	Electricity	Solar Irradiance
Minimum	0.673	0.0171	0.0267
1st Quartile	0.770	0.0510	0.0799
Median (2nd Quartile)	**0.797**	**0.0905**	**0.106**
3rd Quartile	0.837	0.119	0.129
Maximum	0.882	0.203	0.278

This analysis has shown that approximately 80% of the internal temperature response of the house is due to the time variant external temperature. Electricity and solar gains being only responsible for 9% and 10% when averaged over the 28 homes.

2.6 Heat wave form

Having concluded that (a) it is possible to fit LPMs very accurately to the measured data; and (b) that the internal temperature response of the buildings during a heat wave is dominated by changes in the external air temperature, not changes in the solar or electric gains for a given building, we now need to consider the form of typical heat waves. We use data from the UK, but the approach could be used for other locations. We term the increase in internal temperature during a heat wave the internal temperature anomaly (ITA). LPMs are linear systems, and

therefore, the period of any output has to be formed from an input with the same wavelength. It is therefore necessary to understand the form of real external heat waves to make sure that the ITAs we select are realistic. As stated previously, it is common in the UK to define a hot event as one where the maximum daily temperature is greater than 5°C above the average maximum summer temperature. Data from London Heathrow in the period from 1961 to 1990 was used to extract heat waves using the previous definition. Although the definition is one of many, it was believed to be sufficient to select the most significant ones, and with them, make a study about the shape of heat waves. If we study the probability of the extracted heat waves using data from London Heathrow (Met Office, 2006) (where the average summer maximum is the mean for the period 1961-1990) we obtain Figure 7 and Figure 8.

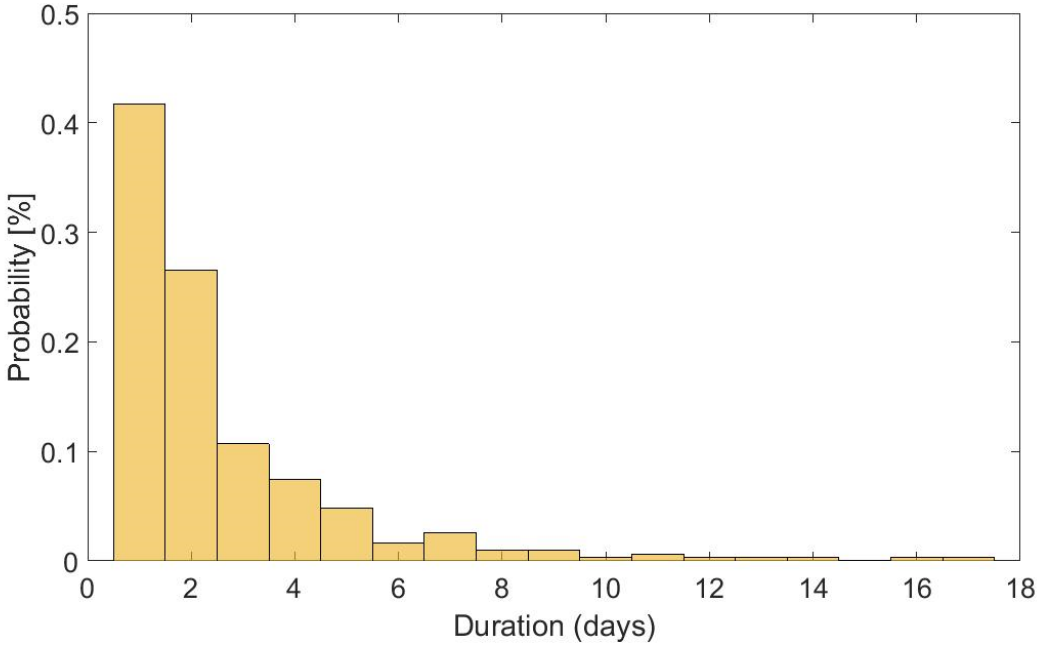

Figure 7. Duration of heat waves in UK.

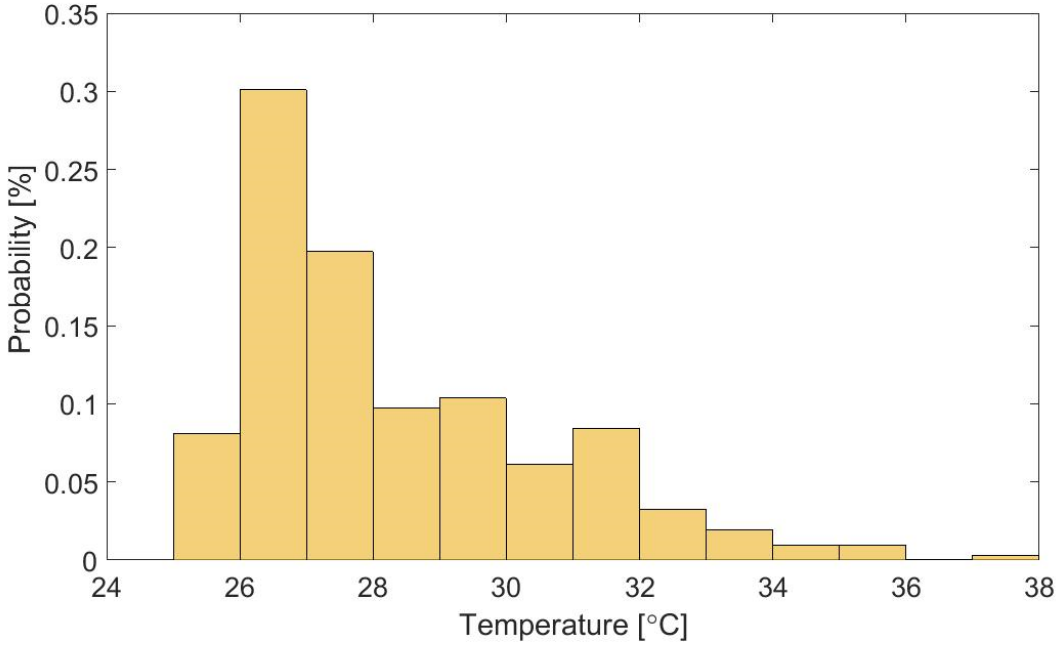

Figure 8. Intensity of heat waves in UK.

In total, 309 heat waves are found. These heat waves have a mean intensity of 28.3°C and a mean duration of 2.6 days.

The London summer base temperature[1] is found to be 20.6°C (from the data previously cited) between 1961 and 1990. The heat waves are then characterized by excursions above the base of between 5.1°C and 16.7°C, with a mean of 7.7°C.

There remains the temporal form of the heat wave. Buildings are natural low-pass filters, so for the methodology to be realistic the real heat waves do not need to be perfectly sinusoidal for the method to work. However, they do need to still contain a smooth hill, particularly in terms of skewness or sharpness. To evaluate that, we have extracted the form of 32 real heat waves. Figure 9 plots 32 random one out of the 309 heat waves from the years between 1961 and 1990 derived from data from (Met Office, 2006). These real heat waves were normalized in time and magnitude to keep only the shape of the actual lift. Once this was done, all of them were plotted (Figure 10), and the average of all of them calculated and plotted (also in Figure 10). This shows the average form of the 28 heat waves once the daily harmonic has been removed. It is clear that the external heat waves are on average rather smooth functions (the black line in Figure 10). Hence, we need a form of synthetic heat wave that also has a diurnal cycle and is smooth. This fits well with the need to drive the LPMs with a simple function, such as a sine wave, in order to arrive at an analytical solution.

[1] Mean temperature of the period between the two equinoxes

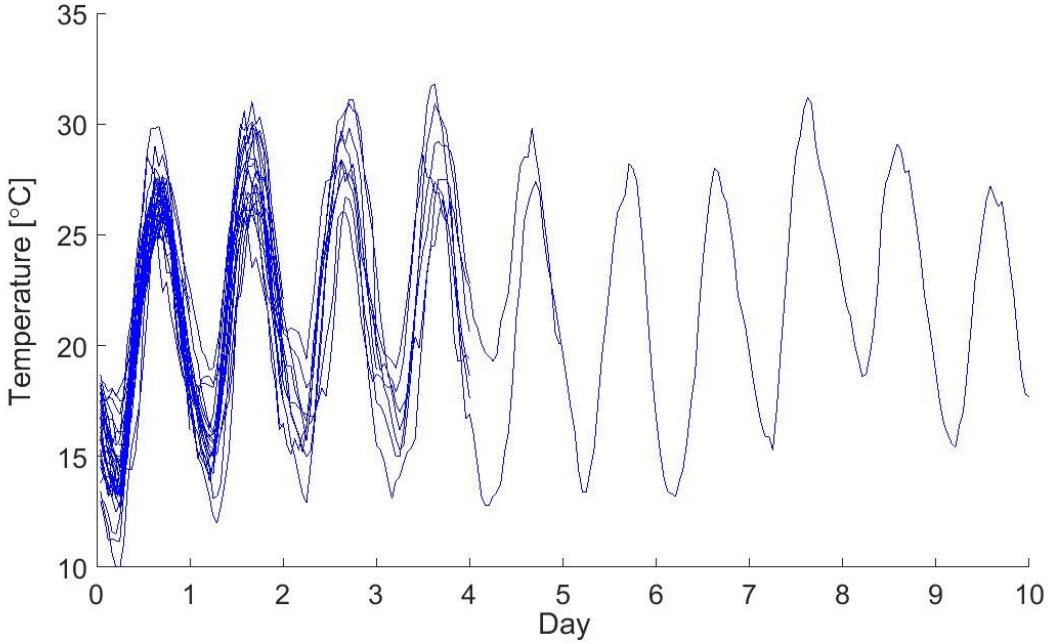

Figure 9. Superposition of 32 UK heat waves with different lengths and intensities from 1961 to 1990.

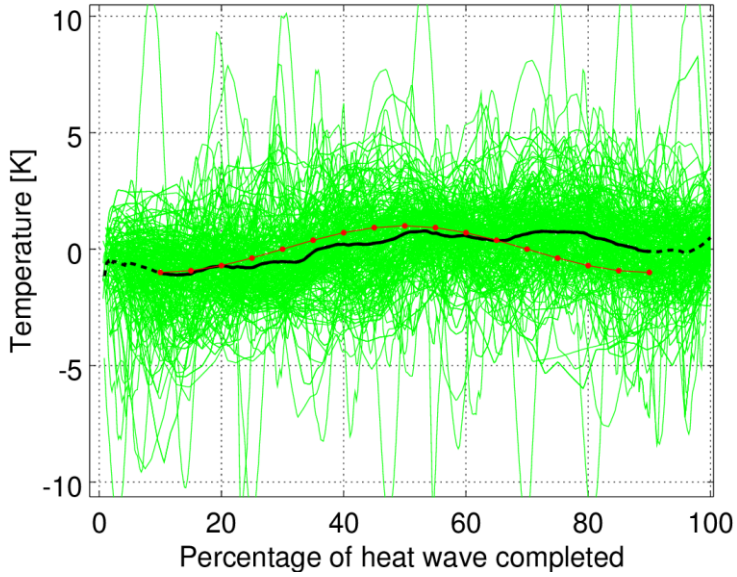

Figure 10. In black, the shape of average heat wave anomaly once the daily harmonic is removed and average temperature and length is normalised. The dashed portions of the black line represent the 10% edges of the curve where transitional effects may come into play. The green lines are each anomaly, and the red line is an example of the shape used in this paper as a synthetic heat wave.

2.7 Selection of synthetic internal anomalies

For synthetic heat waves to be of use in any dialogue between designer and client, and to have real meaning to the public when used to declare a health emergency, these heat waves need to be describable in simple terms. For example, a heat wave of "5°C above normal for 5 days". The methodology though, needs to define the heat wave as a smooth rise in the temperature - as seen in the previous section. Inconveniently, a half sine wave of height 5°C and a width of 5 days, is only momentarily at 5°C, and hence does not match the natural description. An obvious solution that fits well with the need to (a) provide a form that gives an analytical solution under an LPM, and (b) can be described in simple public-orientated terms is to describe/classify the hump in terms of a rectangle that fits within it (see Table 3 for examples). This approach also fits well with the data shown in Figure 9 and Figure 10 and with the UK Met Office description of a heat wave given in the introduction. The sinusoidal chosen is the one that fully encloses the pulse (defined for example as 5°C above normal for 5 days) yet has minimum area. This can be achieved in all cases by multiplying the stated duration by 2.381 and the amplitude by 1.602.

Table 3: A selection of ITAs (the sinusoidal forms) and their public-orientated descriptors (the rectangular forms).

	Duration 3 Days	Duration 5 Days	Duration 7 Days
Intensity +2 kelvin	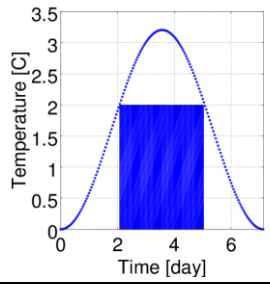	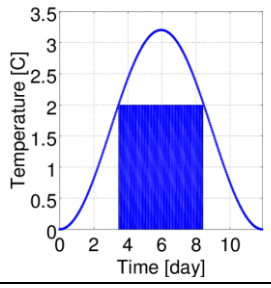	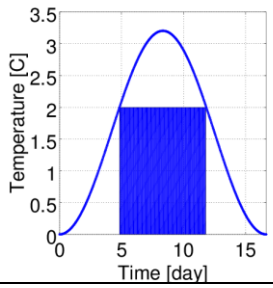
Intensity +4 kelvin	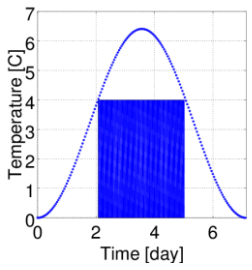	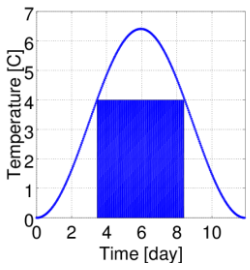	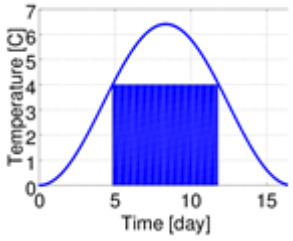

Intensity +6 kelvin	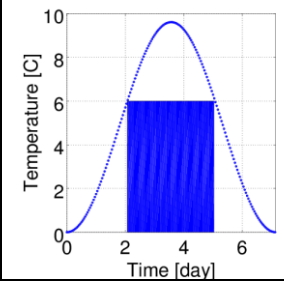	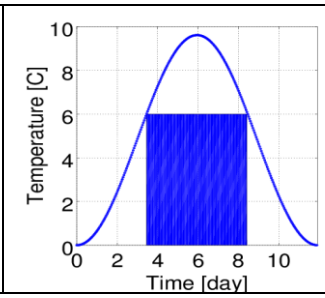	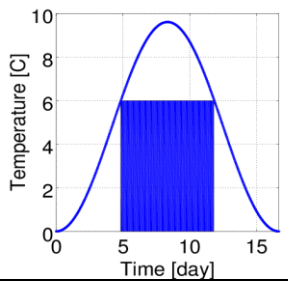

Table 4: Nomenclature for the ITAs shown in Table 3 and used in the results section.

Duration	Intensity		
	A = +2 K	B= +4 K	C = +6 K
3 days	A3	B3	C3
5 days	A5	B5	C5
7 days	A7	B7	C7

Table 5: Consequences of the ITAs on complaints about overheating in commercial buildings per square meter of floor area with ITAs being over imposed to the comfort limit of 24 Celsius according to Federspiel (Federspiel et al 1998).

Duration	Intensity		
	A = +2 K	B= +4 K	C = +6 K
3 days	0.19	0.83	2.16
5 days	0.32	1.39	3.60
7 days	0.45	1.94	5.04

Table 4 shows the targeted internal temperature anomalies. We now need to find the external temperature anomalies or synthetic heat waves (SHWs) that would give rise to these ITAs in buildings, i.e. to reverse engineer the external heat waves. This is the core of this work: to reverse engineer heat waves, that give predefined internal conditions that might be of concern to public health. That ITAs of this magnitude have a material effect on occupants is shown in Table 5, which shows the impact of the ITAs on building occupants according to the model of Federspiel (Federspiel et al 1998). In their study, Federspiel et al. performed a detailed study on how absolute temperatures outside of the comfort limits for a given length of time represent dissatisfaction in building occupants. The ITAs in this paper have been chosen in a way in which they cover a substantial range of extreme events in the interior of the building. We checked the range of discomforted people they generate according to the Federspiel model. The result showed

that the ITAs cover the range from very low dissatisfaction, to very high dissatisfaction. We used this as a check for verifying that the ITAs chosen were adequate.

We undertake the reverse engineering using the 28 LPMs of the monitored homes. As each one of the houses has a different thermodynamic response, each one of the houses will need a different SHW to produce the same ITA.

Our ITAs (Table 3) are sinusoidal functions defined on the interval -π/2 to 3π/2, and shifted by a positive factor equal to its amplitude to ensure that all the values are positive:

$$\mathrm{ITA}(t) = 1.602 \times 0.5 \times A\left(1 + sin\left(\frac{2\pi t}{2.381T} - \frac{\pi}{2}\right)\right)$$	Eq. 2

with *A* the amplitude of the ITA in kelvin, t time in hours and T the length of the ITA in hours.

In a dynamic linear system, a sinusoidal input has a sinusoidal output with the same angular frequency but different amplitude and with a lag. The attenuation factor and the lag can be obtained by the transformation of the transfer function to the Laplace domain. The Laplace domain allows one to transform the differential equations governing the system into algebraic equations defined on the frequency domain. However, this is only true if the system has been given enough time to adapt to the given cyclic driving force. In our case, the excitation only occurs for one cycle, this implies that the input for generation of the ITA, has to include a factor accounting for the transitory effect. This is the transient component, and its magnitude is rather small, and it can be found using systems theory (Ogata 2009). The models we use have order three, meaning the transfer function that relates the outputs and inputs also has order three.

An LPM can be represented in the Laplace domain as a transfer function between an input (the external temperature) and the output (the internal temperature). In the Laplace domain, the frequency is the independent variable, and the attenuation of the transfer function and lag, depend on it. The transfer function used is given by Eq 3. The transfer function is given in fractional form, and the response of the system is highly conditioned by the values of frequency at which the denominator is made zero. These are called the poles of the system and provide information about the dynamic response of the system. . The poles with absolute values closer to zero are considered the most dominating poles of the system as they have the biggest influence on the response (Ogata, 2009).

$$\mathrm{H(s)} = \frac{\mathrm{K}*(\mathrm{s}-\mathrm{z}_1)*(\mathrm{s}-\mathrm{z}_2)}{(\mathrm{s}-\mathrm{p}_1)(\mathrm{s}-\mathrm{p}_2)(\mathrm{s}-\mathrm{p}_3)}$$	Eq. 3

In this equation z_1 and z_2 represent the frequencies that make the transfer function's numerator zero, and p_1, p_2 and p_3 represent the poles of the system.

Knowing that a relationship between the most dominant pole and the error due to the transitory effects in the model will provide a good adjustment, a correction factor was obtained via the correlation found between the value of the dominant pole and the error due to the transitory effects, via Eq 4.

$$\mathrm{MAG} = \mathrm{MAG}_{ssr}\left(0.9829 + 0.0021\frac{1}{|\mathrm{pole\_min}|}\right) \quad \text{Eq. 4}$$

Where MAG_{ssr} is the magnification obtained from the Bode diagram and valid for the stationary sinusoidal regime (SSR), and MAG is the magnification needed to produce an accurate ITA.

The above was used to identify the magnitude modification that the transitory regime may have on the SHW. However, when evaluating the lag that the SHW has to have to produce the given ITA the method is simpler, as the time difference between input and output is not affected by the transitory part of the response. It is therefore possible from the Laplace domain to obtain the lag between the input and the output using the wave length of the ITA under study and by calculating the phase of the transfer function.

From the above it is now possible to calculate analytically the magnification and lag that is needed to generate an SHW that will produce a given ITA. If the ITA has the form shown in Eq. 2. Then the SHW that will generate that ITA should have the form:

$$\mathrm{SHW(t)} = 1.6027\,\mathrm{MAG} \times 0.5\,\mathrm{A}\left(1 + \sin\left(2\pi\frac{t-PHA}{2.381\mathrm{T}} - \frac{\pi}{2}\right)\right) \quad \text{Eq. 5}$$

With PHA being the lag (in hours) between input and output obtained analytically from the transfer function of the system.

3 Results

Each of the 28 buildings produces a different SHW for any ITA in Table 4. The aim of this work is to create a methodology that allows one to obtain a single SHW or a small set of SHWs that can serve as a resilience check of buildings. This suggests we seek SHWs that would, for example, give rise to temperatures of greater than X for more than Y hours in Z percent of the stock. Plotting the amplitude of the SHWs generated by the above method for our stock of 28 buildings gives Figure 11.

Once it has been decided what increase in internal temperature is considered pernicious, one can use the method presented here to create the heat wave that will give rise to this increase. As different buildings will "suffer" differently in the event of a given heat wave, each building will have a different synthetic heat wave that will produce a given ITA, it is therefore necessary to also state what percentage of homes it is considered unacceptable to suffer the given internal anomaly. These two parameters then allow the generation of a synthetic heat wave that will produce at least that anomaly for that percentage of homes.

Referring to Figure 11, if one wants to find the SHW that would generate an ITA of duration 4 days with an intensity of 2K in 75% of UK houses (assuming our sample of 28 is reasonably representative), one begins by determining the magnification for 4 days in 75% of the stock. This is achieved by following the red arrows in Figure 11, to obtain a magnification of 1.42. This magnification will be the same regardless of the intensity of the ITA. Hence the external temperature amplitude will be 1.42 times 2 kelvin. The equation for the SHW will then be in this case:

$$\mathrm{SHW} = 1.42 \times 1.6017 \times 0.5 \times 2[\mathrm{kelvin}]\left(1 + \sin\left(2\pi\frac{t - 6.48}{2.381 \times 96[\mathrm{hours}]} - \frac{\pi}{2}\right)\right)$$

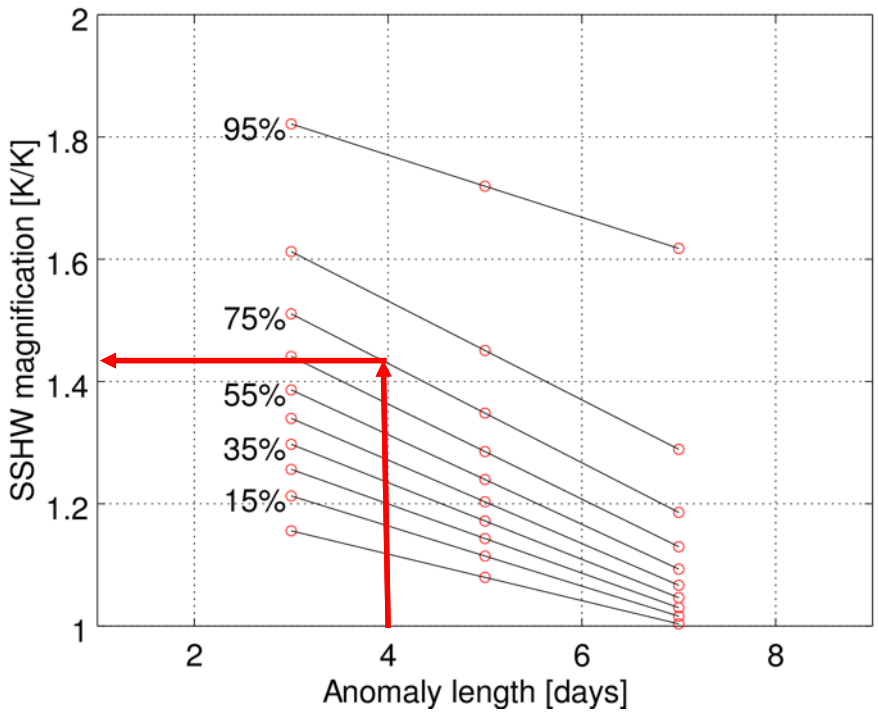

Figure 11. Chart to derive the SHWs' amplitude (as a multiplier of the ITA amplitude) based on the duration of the ITA. The percentage is the percentage of the building stock affected to at least this degree.

In the same way it is possible to obtain the lag (the number of hours between when the SHW peaks and the ITA peaks) that will be seen between the SHW and the ITA. This parameter may be of interest to those designing actuation plans for heat waves as it provides a warning period. For example, using Figure 12, and starting from the duration of the ITA on the x-axis, a vertical line followed to the line that represents 75% of the buildings. The Y-axis then gives the lag, in this case 0.27 days (6 and half hours). Table 6 gives example values for three of the ITAs in Table 4. It should be noted in this table that the standard deviations are large in the case of the magnification among buildings, but not in the case of the lag. This implies that different houses will be affected by heat waves in different ways, and that the variability between homes will be larger than the variability that an average home will have between different anomalies (A3, A5 and A7). This is why this study was interesting, it is crucial to understand the building stock in its variability to have valuable findings. The lag however, is much more constant between homes, and it is the different anomalies what produce different lags in their effects.

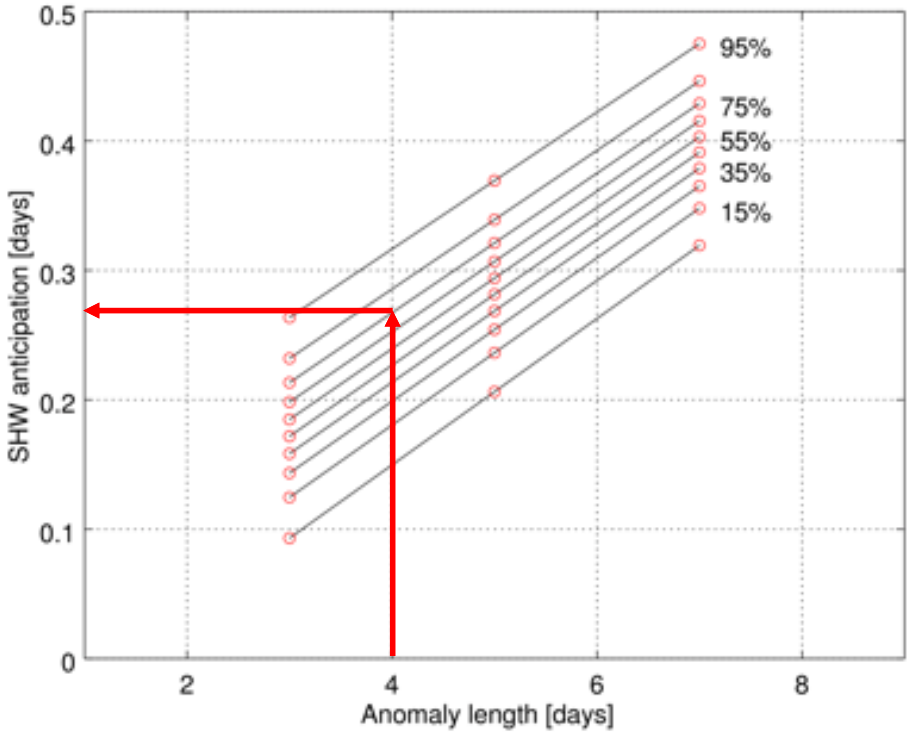

Figure 12. Chart used to derive SHWs' lag based on the length of the ITA.

Table 6. Relationships between ITAs from group A and SHWs.

ITA	SHW

Anomaly	Intensity [K]	Duration [days]	Mean magnification (50% of homes) [K/K]	Standard deviation of Magnification due to homes variability [K/K]	Mean lag (50% of homes) [days]	Standard deviation of lag due to homes variability [days]
A3	+2	3	1.3772	2.6307	0.36749	0.05108
A5	+2	5	1.1956	3.1486	0.61161	0.04963
A7	+2	7	1.0899	4.0612	0.79203	0.05411

4 Validation of the method

As the results presented so far are based on measured data they are validated for the 28 homes considered. What remains to be confirmed is the correctness and utility of the method. This is best achieved by applying the newly created SHWs to buildings as they would be modelled by researchers or practicing engineers, using benchmark software tools. We chose to test the A3 ITA as the process is the same for all SHWs. In order to do this, a suitable weather file was created by superimposing the SHW given by A3 onto a synthetic weather file consisting of a flat temperature signal with amplitude of 20ºC and all the other weather variables made constant (by setting them to their annual average) except for the solar gains that were set to zero, as this gain will have no influence in this particular comparison. The Synthetic Heat Waves Weather Files proposed here are to be taken as a definition per se of several heat waves. A definition that is derived by the effect that they have in our population considering the current building stock. And with this establish a benchmark in the same way as the 1990 figures of CO_2 emissions stablish a baseline when discussing energy use. Our synthetic weather files would contain a variety of Synthetic Heat Waves that have a given effect on the Building Stock of 2006. This would could be updated as the building stock is (hopefully) improved.

We then created a SHW that would produce at least an A3 (i.e. a 2K rise for 3 days) in 50% of the dwellings (we term this A3/50). For that we use the graph in Figure 11 and Figure 12 so we can evaluate the lag that we would expect between SHW and ITA.

Each of the 28 buildings used to obtain the LPMs were modelled in Energy Plus (a construction industry standard for thermal simulation - see the Appendix 3 for construction details and modelling assumptions) under this SHW. The SHW was placed starting at day 30 of the simulation to ensure a warm up period. The results are shown in Figure 13.

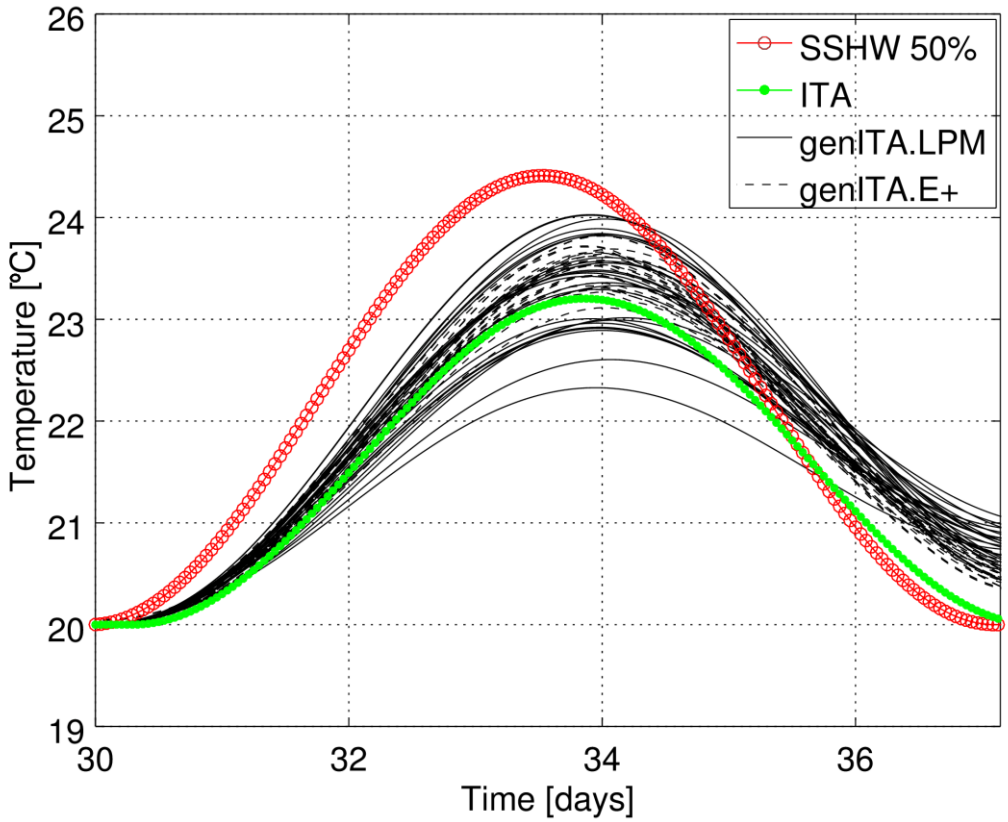

Figure 13. Impact of the SHW A3/50 on the 28 buildings given by an A3 ITA when modelled in EnergyPlus (genITA.E+) and modelled with LPM (genITA.LPM).

We can see in Figure 13 how the models from EnergyPlus also show a temperature rise and duration similar to the ITA. This implies that the method produced similar results when used within industry standard software, not just within LPMs. We see that 85.7% have elevated temperatures of at least 2K for at least 3 days. This is more than the 50% required, indicating the method is conservative. It is also worth noting that as the EnergyPlus models were created using data from the SAP assessment of the buildings. This is known to be imprecise, so we would not expect perfect fidelity.

Also, after consideration of this graph, one has to take into account that several works in the literature where the European Energy Performance Certificate (a European equivalent with respect to methodology of calculation and purpose) has failed to provide an accurate performance evaluation with respect to overall heat transfer of the building (Tronchin et al. 2012), (Herrando et al. 2016) or (Iman et al 2017). It is for this reason that we did not want to give too much importance to the extract comparison between these two sets of models. It was just to show that we are seeing similar responses between the two. The reader is invited to examine Appendix 1 and Appendix 3 to identify differences between the HTCs derived from the SAP evaluation

(visual inspection tests), and the conductivities derived from the data (therefore correct by design) to find the reason for the discrepancies in the curves of Figure 13.

5 Example of the synthetic heat waves for practitioners

The temperatures found within a building during a heat wave will be a complex product of the interaction of the architecture, the occupants and the local weather. Although it would be easy to splice the SHWs into a time series of observed weather, or a test reference year (Eames et al. 2010), this would raise questions of where exactly in the year to place it and what the impact of the weather just before the SHW might be, and it would be hard to find a consistent solution for all locations. For example, picking a date such as the 1st July would not work, as in one location the week before might have been particularly hot, but in another not so. Hence we suggest the use of totally synthetic weather during the run-up period based on simple functions for all variables when trying to quantify the resilience of a building or a design to heat waves in a robust and consistent way. Clearly this is an approximation, similar in some ways to the admittance method (Clarke, 1985) but we are trying to rank-order the resilience of designs so it would seem reasonable. The most critical time series would be the temperature time series and we suggest that this is constructed using a sine wave with a 24-hour period, with the mean equal to the summer time mean over a twenty-year period and the diurnal cycle also being the mean over this period. As these numbers are known for future years from climate change modelling, researchers should also be able to use the approach to look at resilience into the future. The other weather variables are slightly more problematic, in that their forms are interlinked, for example humidity is related in many locations to temperature. It is not known whether this interlinking is material for this kind of work, but it is likely that all the necessary weather variables can be represented by simple forms even if they are interrelated.

We term such a SHW embedded within a weather time series produced using simple synthetic time series for all variables, a super synthetic heat wave (SSHW). Figure 14 shows the A3/50 example for Nottingham with the mean and diurnal cycle based on the 20 years of observed weather (astronomical summer) used to assemble the current test reference year for Nottingham. As can be seen, the heat wave becomes an uplift to the normal diurnal signal.

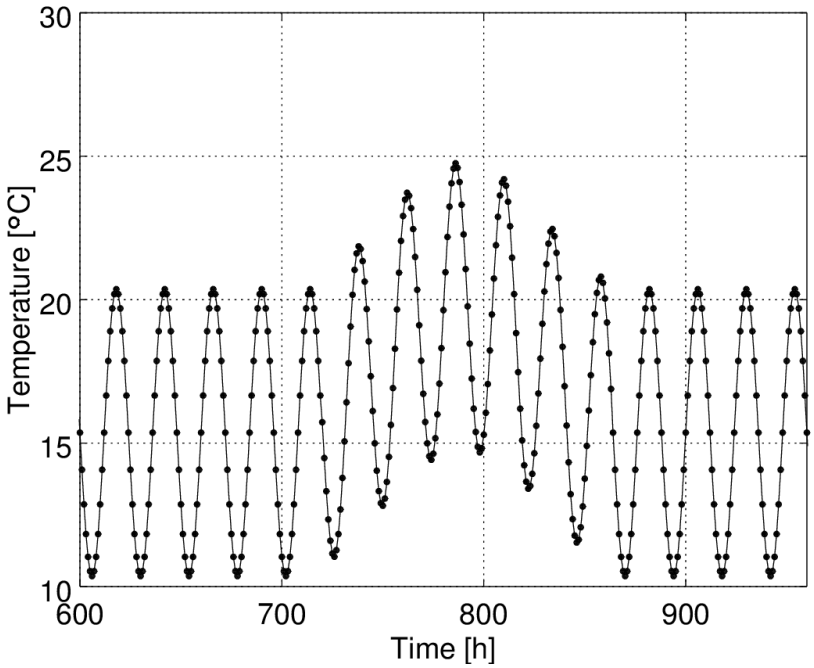

Figure 14. A3/50 SSHW for Nottingham.

If we assume ranges of possible heat wave durations of at least 3 to 7 days (as indicated by Table 5) and the range of amplitudes to be 2 to 6 °C (as indicated by Table 5) we have 25 possible combinations, even if we restrict ourselves to integer values of duration and amplitude. It is unlikely either researchers or practicing engineers would be interested in all possible combinations, hence we suggest that the reduced escalating set of five SHWs shown in Table 7 might be useful for comparing the resilience of designs, however other sets could be used. This set and its nomenclature has been picked to have resonance and simple meaning with architects, designers, government and the public. The methodology presented here aims at providing the scientific tools to create synthetic heat waves that will help with the analysis of resilience. Depending on the application at hand, the professionals in charge of designing the synthetic weather-files (policy makers or professional associations), will determine the ITAs, after considering the effect in the population that they are willing to accept. This will include the effect on occupants (ITAs) and the maximum percentage of homes that it is considered reasonable to suffer a particular ITA. Here we provide two examples to illustrate the application, but each application of the method can have a variety of approaches. In this case two percentiles have been chosen. One (50%) indicating that half or more buildings will show such an increase above typical for the time of year. The other, indicating 10% of buildings will show such an increase, being more precautionary, as it is presumably often unknown in what housing vulnerable groups

might be resident. 10% will also be of use to those wanting to show that their design is particularly resilient to heat waves, as it indicates that 90% of building fare worse.

Table 7. Suggested list and nomenclature of possible SHWs for studying resilience. For example, the heat wave shown in bold would be referred to simply as "2/10".

Rise (°C)	Percentile	Meaning of heat wave
2	**10**	**A 2°C rise in temp above normal for 2 days in 10% of buildings**
2	50	A 2°C rise in temp above normal for 2 days in 50% of buildings
4	10	A 4°C rise in temp above normal for 4 days in 10% of buildings
4	50	A 4°C rise in temp above normal for 4 days in 50% of buildings
6	10	A 6°C rise in temp above normal for 6 days in 10% of buildings
6	50	A 6°C rise in temp above normal for 6 days in 50% of buildings
8	10	An 8°C rise in temp above normal for 8 days in 10% of buildings
8	50	An 8°C rise in temp above normal for 8 days in 50% of buildings
10	10	A 10°C rise in temp above normal for 10 days in 10% of buildings
10	50	A 10°C rise in temp above normal for 10 days in 50% of buildings

With future knowledge of return periods for such events, additional meaning could be given to the SHWs, for example that in London SHW 4/10 has as return period of X years, now and Y in 2080.

In practice, it is envisioned designers would apply the SSHW of interest, for example the 4/10, within a dynamic thermal model of their building, and if their design did not increase (in this case) by 4°C for 4 days, then it is more resilient to such a heat wave than 90% of the domestic stock, thereby providing confidence. The idea will be that the users of this methodology will know that the effect of the synthetic weather is the one that would occur in a 2006 building stock. The effects in current and future stock will have to be re-calculated, as is done in other methodologies such as the future climate predictions for creating future weather files.

Alongside testing a design against the pre-existing stock, there is the need to test against targets that reflect the potential to cause discomfort or harm. Hence, further work is needed to understand the implications of maintaining vulnerable groups at high temperatures for differing periods of time within buildings.

It is possible that 28 buildings might not be enough to statistically represent the full range of domestic buildings that exist. However, this number could be increased at very low cost, and there may already be larger data sets of internal temperature time series that could be used.

6 Summary and Conclusions

Previous definitions of heat waves have all been based on external conditions, yet it is the conditions within buildings that kill people, often in large numbers. In this work, we have developed a way of defining heat waves in terms of the impact they would have on conditions within buildings and on their occupants. This was based on data collected in 28 dwellings during a heat wave. The buildings used are from four different locations in the UK. The buildings' characteristics are detailed in Appendix 1, and they have been picked randomly from a published database. The buildings are representative of the UK stock, but the methodology that we present can (and should be) applied world-wide, thereby giving synthetic heat waves that are truly occupant-centric. Considering that many countries have initiatives to capture and record energy consumption and other environmental parameters such as temperatures, one can anticipate that the methodology could easily be applied internationally.

As part of this, we converted a problem that needs to be solved in a numerical way building-by-building, into a general analytical problem. The final result is a set of super synthetic heat waves that can be used to discuss and rank order the resilience of new buildings or pre-existing ones, or to set alerts for public emergencies.

The work uses a methodology that employs data-driven models that have been created to fit the behaviour of real buildings, this should be contrasted with models created from architectural drawings—which are known to frequently not represent a building as-built (especially with respect to air tightness and U-value), nor to contain a truthful description of how the occupants really use the building. Although the models used are simpler than industry standard models such as Energy Plus, they offer the certainty of fitting the real world by default. More importantly, they also offer the advantage of having analytical forms that allow one to not

only obtain the output (internal conditions) for a given input (weather data, etc.) but also to reverse the process.

The method used for this reverse engineering consisted of using systems theory and Laplace domain modelling analysis to identify the external heat waves that produce a defined internal temperature response within the buildings. The method was shown to be accurate and produced results consistent with those from Energy Plus—which is important if the super synthetic heat waves are to be adopted as one method of showing compliance to a regulatory body. The method was also shown to be easy to use, as it can be reduced to consulting a graph, or using an algebraic equation. We were then able to create synthetic heat waves that produce an internal overheating defined by us within a set percentage of the building stock. This is the core result of the paper, and it has the potential to alter the way we assess the resilience of buildings.

In addition, the form of the heat waves produced were shown to be similar to those from observed heat waves. This suggests that they could also be of use to those wanting to look at the resilience in other settings, for example cladding materials or agriculture.

By exchanging an external definition of a heat wave for an internal one, we believe the method is a more human-centric way of evaluating the resilience of buildings, and could form the basis of an early warning system for declaring a health emergency.

For those wishing to try the approach, SSWHs in epw format can be downloaded from colbe.bath.ac.uk.

7 Acknowledgements and data access

This research was carried out as part of the EPSRC funded projects: COLBE (The Creation of Localized and Future Weather for the Build Environment, EP/M021890/1); Zero Peak Energy Building Design for India (ZED-i) EP/R008612/1 and Active Building Centre EP/S016627/1. The data used in this project can be found at doi

8 References

Bacher, P. and H. Madsen (2011). "Identifying suitable models for the heat dynamics of buildings." Energy and Buildings 43(7): 1511-1522.

BOM (2013). Extreme Heat Services for South Australia. J. R. J. 2013.

Carbon Trust. Micro-CHP Accelerator Final Report – March 2011. Richard Guy and Benjamin Sykes. United Kingdom 2011.

CIBSE (2006). Guide A: Environmental design. London, The Chartered Institution of Building Services Engineers.

Clarke, J. A., Energy Simulation in Building Design (1985) Butterworth-Heinemann, London.

CLG (2007). English House Condition Survey, Annual report, Communities and Local Government.

Coley, D. A. and J. M. Penman (1992). "2nd-Order System-Identification in the Thermal Response of Real Buildings .2. Recursive Formulation for Online Building Energy Management and Control." Building and Environment 27(3): 269-277.

Coley, D. and T. Kershaw (2010). "Changes in internal temperatures within the built environment as a response to a changing climate." Building and Environment 45(1): 89-93.

DMI (2013). Danmark får varme- og hedebølge (In Danish). D. M. I. J. R. J. 2013.

Eames, M., T. Kershaw and D. Coley (2011). "On the creation of future probabilistic design weather years from UKCP09." Building Services Engineering Research and Technology 32(2): 127-142.

Eames, M., T. Kershaw and D. Coley (2011). "The appropriate spatial resolution of future weather files for building simulation." Journal of Building Performance Simulation 5: 1-12.

Federspiel, C.C. 1998. Statistical analysis of unsolicited thermal sensation complaints in commercial buildings. ASHRAE Transactions 104 (1). 912-923.

Fraisse, G., C. Viardot, O. Lafabrie and G. Achard (2002). "Development of a simplified and accurate building model based on electrical analogy." Energy and Buildings 34(10): 1017-1031.

Guan, L. (2009). "Preparation of future weather data to study the impact of climate change on buildings." Building and Environment 44(4): 793-800.

Herrando, M., Cambra, D., Navarro, M., de la Cruz, L., Millan, G., Zabalza, I., Energy performance certification of Faculty Buildings in Spain: The gap between estimated and real energy consumption. Energy Conversion and Management 125 (2016) 141-153.

Iman, S., Coley D.A., Walker, I., The buiding performance gap: Are modellers literate? Building Services Engineering Research and Technology 38(3) (2017) 351-375.

IPCC, 2014: Climate Change 2014: Synthesis Report. Contribution of Working Groups I, II and III to the Fifth Assessment Report of the Intergovernmental Panel on Climate Change [Core Writing Team, R.K. Pachauri and L.A. Meyer (eds.)]. IPCC, Geneva, Switzerland, 151 pp.

Jentsch, M. F., A. S. Bahaj and P. A. B. James (2008). "Climate change future proofing of buildings—Generation and assessment of building simulation weather files." Energy and Buildings 40(12): 2148-2168.

Jentsch, M. F., P. A. B. James, L. Bourikas and A. S. Bahaj (2013). "Transforming existing weather data for worldwide locations to enable energy and building performance simulation under future climates." Renewable Energy 55: 514-524.

Kershaw, T., M. Eames and D. Coley (2011). "Assessing the risk of climate change for buildings: A comparison between multi-year and probabilistic reference year simulations." Building and Environment 46(6): 1303-1308.

Madsen, H. and J. Holst (1995). "Estimation of continuous-time models for the heat dynamics of a building." Energy and Buildings 22(1): 67-79.

Malisani, P., F. Chaplais, N. Petit and D. Feldmann (2010). "Thermal building model identification using time-scaled identification methods." 49th Ieee Conference on Decision and Control (Cdc): 308-315.

Meehl, G. A. and C. Tebaldi (2004). "More intense, more frequent, and longer lasting heat waves in the 21st century." Science 305(5686): 994-997.

Ménézo, C., J. J. Roux and J. Virgone (2002). "Modelling heat transfers in building by coupling reduced-order models." Building and Environment 37(2): 133-144.

Met Office (2006): MIDAS: UK Hourly Weather Observation Data. NCAS British Atmospheric Data Centre, 06-2019. http://catalogue.ceda.ac.uk/uuid/916ac4bbc46f7685ae9a5e10451bae7c

Monteiro, A., Carvalho, V., Oliveira, T., Sousa, C., "Excess mortality and morbidity during the July 2006 heat wave in Porto, Portugal." Journal of Biometeorology 57:155-167.

Muneer, T. (1990). "Solar radiation model for Europe." Building Services Engineering Research and Technology 11(4): 153-163.

NWS, 2019. Heat - A Weather Hazard of Summer. National Weather Service, https://www.weather.gov/btv/heat_awareness. Accessed 27/09/2019.

Ogata, K. (2002). Modern Control Engineering. Upper Saddle River, New Jersey, Prentice Hall.

Pilkington B, Roach R, Perkins J (2011) Relative benefits of technology and occupant behaviour in moving towards a more energy efficient, sustainable housing paradigm. Energy Policy 39:4962–4970.

Ramallo-González, A. P.; Brown, M.; Gabe-Thomas, E.; Lovett, T. & Coley, D. A. (2018), 'The reliability of inverse modelling for the wide scale characterization of the thermal properties of buildings', Journal of Building Performance Simulation 11(1), 65-83.

Robinson, P. J. (2001). "On the Definition of a Heat Wave." Journal of Applied Meteorology 40(4): 762-775.

Russo, S., Sillman, J., Fischer, E. M., (2015). "Top ten European heatwaves since 1950 and their occurrence in the coming decades." Environmental Research Letters 10(12): 124003.

SMIH (2013). Värmebölja | Klimat | Kunskapsbanken | SMHI (in Swedish). R. J. 2013.

Stott, P. A., D. A. Stone and M. R. Allen (2004). "Human contribution to the European heatwave of 2003." Nature 432(7017): 610-614.

Tindale, A., (1993). "Third-order lumped-parameter simulation method." Building Services Engineering Research and Technology 14 (3): 87-97

Tronchin, L., Fabbri, K., Energy Performance Certificate of building and confidence interval in assessment: An Italian case study. Energy Policy 48 (2012) 176-184.

Xu, X. H. and S. W. Wang (2007). "Optimal simplified thermal models of building envelope based on frequency domain regression using genetic algorithm." Energy and Buildings 39(5): 525-536.

Zampieri, M., S. Russo, S. di Sabatino, M. Michetti, E. Scoccimarro and S. Gualdi (2016). "Global assessment of heat wave magnitudes from 1901 to 2010 and implications for the river discharge of the Alps." Science of The Total Environment 571: 1330-1339.

9 Appendix 1. Building Narratives

	District	Fl. Area [m2]	Archetype	Year	Wall Area [m2]	Wall U-Value	Glass Area [m2]
1	Belfast	31.20	3rd floor of Mid Terrace	1904	67.84	3.26	7.7
2	Manchester	85.00	Mid Terrace	2006	57.77	0.20	19.7
3	Manchester	85.00	Mid Terrace	2006	57.77	0.20	19.7
4	Manchester	85.00	Mid Terrace	2006	57.77	0.20	19.7
5	Nottingham	93.91	Detached Cottage	1790	107.67	0.90	22.8
6	Nottingham	90.26	Semi Detached	1957	71.56	2.12	25.6
7	Belfast	77.17	End Terrace	1959	97.60	0.76	17.9
8	Belfast	65.62	Semi Detached	1924	missing	missing	10.3
9	Belfast	64.86	3rd floor of Mid Terrace	1904	missing	missing	9.9
10	Belfast	61.33	Semi Detached	1969	73.68	missing	4.3
11	Belfast	94.06	Semi Detached	2005	missing	missing	20.1
12	Belfast	88.00	End Terrace	1964	88.46	1.63	14.0
13	Belfast	57.22	Mid Terrace	1904	missing	missing	5.0
14	Belfast	88.80	End Terrace	1960	89.87	0.62	13.5
15	Cambridge	95.81	End Terrace	2005	78.68	0.63	11.9
16	Belfast	77.80	Semi Detached	1964	108.00	0.46	18.2
17	Belfast	62.52	End Terrace	1969	96.50	0.46	13.3
18	Cambridge	95.81	Mid Terrace	2005	78.68	0.63	11.9
19	Belfast	67.27	3rd floor of Mid Terrace	1904	missing	2.20	7.1
20	Belfast	58.85	Mid Terrace	1969	86.20	0.76	13.5
21	Cambridge	95.81	End Terrace	2005	78.68	0.63	11.9
22	Cambridge	95.81	End Terrace	2005	78.68	0.63	11.9
23	Belfast	75.63	Terrace	1969	97.80	0.46	14.2
24	Belfast	38.66	Mid Terrace	1904	missing	1.20	8.5
25	Cambridge	95.81	End Terrace	2005	78.68	0.63	11.9
26	Derby	41.80	Semi Detached	1970	25.65	0.52	14.0
27	Belfast	77.17	Mid Terrace	1969	97.60	0.76	17.9
28	Belfast	80.90	End Terrace	1959	119.60	0.76	15.2

10 Appendix 2. Lumped Parameter Models

Error on the fitting in CDH. Err = (CDH_sim – CDH_real)/CDH_real

ID	K1 [W/K]	C1 [Wh/K]	K2 [W/K]	C2 [Wh/K]	K3 [W/K]	C3 [Wh/K]	K4 [W/K]	SF	Err
1	191.06	91.13	84.70	143.09	84.18	4982.82	35.48	1.10	0.047731
2	128.95	0.01	69.35	199.65	100.46	5135.95	53.53	3.05	0.112375
3	166.88	62.44	0.00	573.49	162.49	4945.20	118.30	4.90	0.008652
4	877.24	143.03	0.00	153.20	98.57	4866.32	66.74	2.03	0.026029
5	252.92	1.12	174.48	322.52	141.92	4919.55	84.10	2.71	0.043731
6	352.51	3002.51	368.61	734.79	275.16	5169.91	412.54	7.35	0.00826
7	200.21	121.58	78.74	174.16	93.64	4992.06	34.11	0.49	-0.02726
8	200.14	120.89	78.81	174.12	93.90	4992.16	33.96	0.95	0.066735
9	389.02	0.01	236.90	591.17	214.34	5204.82	90.71	2.28	0.031665
10	609.32	0.18	380.08	844.13	563.41	4996.06	167.99	4.24	0.040354
11	146.85	284.72	234.53	273.74	103.54	4947.87	82.43	2.31	0.060598
12	355.74	3005.74	371.84	746.72	278.39	5173.14	420.02	10.58	0.018903
13	451.05	286.63	0.00	495.80	199.70	5039.17	169.35	3.12	0.042976
14	390.77	0.00	148.70	590.50	223.15	5179.46	123.56	2.94	0.078082
15	0.00	131.24	332.01	65.45	68.45	1200.95	81.12	0.25	0.035857
16	500.28	1000.28	366.38	1000.28	272.93	5167.68	201.39	5.12	0.031342
17	255.71	2117.15	56.98	613.05	104.93	5294.83	151.89	1.65	0.024542
18	514.57	314.57	214.57	1014.57	614.57	50014.57	272.83	19.40	0.036825
19	566.67	47.30	157.61	203.25	116.12	4493.08	10.42	1.87	0.029433
20	268.20	314.90	180.29	266.49	105.15	5149.23	62.09	1.73	0.030092
21	200.05	121.05	78.05	174.05	93.05	4992.05	33.27	1.35	0.054055
22	263.84	93.83	109.46	242.55	172.33	4945.35	89.21	1.00	0.044456
23	320.01	0.17	167.93	501.68	131.53	4921.23	0.00	0.96	0.095427
24	158.26	1593.63	247.37	900.80	236.58	5253.78	311.42	3.38	0.047512
25	413.89	0.00	277.80	631.60	233.23	5056.88	77.96	4.00	0.060017
26	461.74	454.55	0.04	112.78	104.64	4896.19	89.20	1.95	0.035728
27	452.64	0.00	156.79	1165.88	320.91	5016.19	234.87	1.41	0.082392
28	976.77	3158.21	342.28	205.38	378.36	2774.62	4.76	2.26	0.130374

11 Appendix 3. Energy Plus models

Three archetypes have been defined to accommodate the building types from which data has been extracted. The three types are detached, semidetached and terrace. Depending on the building type a different configuration will be adopted that will affect the number of walls that are adiabatic and the facades in which windows are located. As shown in Appendix 1, some of the parameters of the buildings are missing. In the case of having a missing value, the average value from the existing values of the other buildings will be adopted.

The process of creating the different buildings have been automated. The floor area was obtained from the building data and always considered that the building had an aspect ratio of 1.5, as there was no information about the aspect ratios.

The ventilation and infiltration of each building was obtained with the SAP Vent HL that is reported on the data. Once transformed in ach considering the volume of the building, a background constant infiltration was considered with that value.

As most of the construction types of walls were unknown, a generic construction with an outer brick layer, and a sandwich configuration with plasterboard – insulation –plasterboard was used. Adjusting the thickness of the insulation it was possible to generate a wall with a U-Value equal to that reported in the data. The same was done with ground floors and roofs.

As no U-Values were provided for windows, generic single, double, and triple glazing windows were used with wooden frame.

The simulation was done using 6 time steps per hour, and the simulation spanned from the first of January to the first of September. Although the output of the simulation only was considered beyond the first of June, the simulation was started from the beginning of the year to make sure that thermal inertia from winter was taken into account in the summer response.

The output of the simulation was the internal temperature of the building that was then used to evaluate and compare with the output from the LPMs.